Large-Scale Confined Gas and Dust Explosions with Elevated Initial Turbulence

Lorenz R. Boeck, C. Regis L. Bauwens, Sergey B. Dorofeev
FM Global, Research Division
Norwood, MA, USA

1 Introduction

Turbulence plays an integral role in the severity of industrial explosions, including explosions of dusts, gases/vapors, and hybrid mixtures. While turbulence can be generated during the course of an explosion due to the interaction of the expansion flow ahead of the flame with surfaces and obstructions [1–3], elevated initial turbulence can play an equally important role [4–6]: Common industrial equipment such as mills, dryers, or reactors, can present inherently turbulent conditions that enhance the effective reactivity of the mixture, resulting in severe explosion hazards. Scenarios involving jet releases or high ventilation rates can similarly pose increased hazards compared to quiescent conditions.

Historically, gas and dust explosion hazards have been evaluated using experimental setups with significantly different levels of initial turbulence. Typically, highly turbulent conditions are present in dust explosions, while gas explosion experiments are most commonly performed under quiescent conditions. This creates considerable uncertainty regarding how to model the contribution of each fuel when both gas and dust are present in a hybrid-mixture explosion. Furthermore, dust explosion reactivity is typically characterized by the deflagration index computed from the maximum rate of pressure rise, while gas explosions are characterized by the laminar and/or turbulent burning velocity.

In this study, the dynamics of turbulent dust and gas explosions are compared under nominally similar levels of initial turbulence, to illustrate the severity of gas explosions under the high levels of initial turbulence that are typically used to characterize dust explosions. In addition, experiments were performed to characterize gas explosions under varying levels of initial turbulence, within the same experimental setup, and compare the scaling of early turbulent burning velocity and maximum rate of pressure rise with initial turbulence. The results from this work will help inform explosion risk assessments and the design of performance tests for explosion protection systems and provide a basis for future studies examining hybrid-mixture explosions involving both gases and dusts.

2 Experimental Setup

Figure 1 shows a schematic of the 8-m^3 explosion vessel used in the present study, equipped with four injectors that create initial turbulence and inject dust as needed. Each injector comprises a 150-L air cannon, a manifold that accepts a dust container, a fast-acting valve that isolates the injector from the

Correspondence to: lorenz.boeck@fmglobal.com

vessel shortly before ignition, and a hemispherical perforated injection nozzle inside the vessel. Gas supply and sampling systems are installed for tests involving gaseous fuels. All mixtures are ignited at the vessel center, using either two Sobbe 5-kJ chemical igniters (for experiments presented in Sec. 3), or a single 100-J electric match (for experiments discussed in Sec. 4).

For dust explosion tests, the dust containers are loaded with the amount of dust required to achieve the desired dust concentration inside the vessel. The air cannons are pressurized, and the vessel is flushed with dry air and partially evacuated prior to each test. The dust is injected by firing the air cannons, increasing the vessel pressure to ambient pressure. All injectors are then automatically isolated from the vessel by closing the fast-acting valves, and ignition is triggered at a defined time ("ignition delay time") measured from the start of injection. The ignition delay time was varied between tests to obtain a range of initial turbulence.

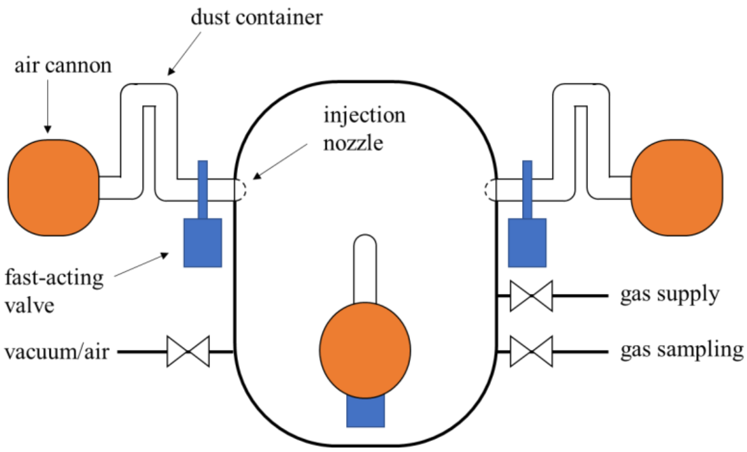

Figure 1: Schematic of 8-m^3 vessel (aspect ratio 1.4) with four injectors and gas supply/sampling.

The procedure for conducting gas explosion tests is similar: The vessel is flushed with dry air, supplied with gaseous fuel, and mixed using a circulation pump. The air cannons are pressurized with air (no dust loaded into the dust containers), and the vessel is partially evacuated. All air cannons are fired to generate turbulence inside the vessel and restore ambient pressure, and ignition is triggered after the desired ignition delay. Since air injection from the air cannons dilutes the fuel-air mixture, the initial mixture contains a pre-calculated fuel concentration that is higher than the final desired concentration. Preliminary testing and gas sampling showed that the desired final fuel concentration is reached with an uncertainty of ±0.1% by volume.

Measurements of vessel pressure during the explosions are taken using a piezoresistive pressure transducer (Kistler 4260A) located at the side of the vessel. Additional transducers near the top and bottom of the vessel are used to verify the measurement. The gas sampling system includes a custom-built infrared absorption measurement and a speed-of-sound measurement (SRS BGA244). Initial turbulence was characterized using a bidirectional probe [7] located at the vessel center, connected to a differential pressure transducer (Setra 239).

3 Comparison of Turbulent Dust and Gas Explosions

A first comparison between turbulent explosions of dust (cornstarch, 750 g/m^3) and gas (propane, 5.0% by volume) is made using two specific ignition delay times, 0.65 s and 0.55 s, and an air cannon pressure of 8.3 bar(g). These parameters are used routinely at the 8-m^3 vessel setup when conducting dust explosion tests with cornstarch. For this dust at a concentration of 750 g/m^3, these ignition delays result in deflagration indices, *K*,

$$K = \left(\frac{dp}{dt}\right)_{\max} V^{1/3} \quad (1)$$

of about 200 and 300 bar·m/s, which represent the upper limits of St1 and St2 dust reactivity classes, respectively. In Eq. (1), $(dp/dt)_{max}$ is the maximum rate of pressure rise measured during the explosion, and V is the vessel volume. Two 5-kJ Sobbe igniters were used as an ignition source (a typical ignition source used for dust explosion testing).

Pressure-time histories and rate of pressure rise curves (60 Hz low-pass filtered) are shown in Fig. 2, along with deflagration indices. Two tests were performed for each condition. Shortening the ignition delay (increasing the turbulent fluctuation velocity) results in faster combustion for both fuels, as expected. The average deflagration indices of turbulent propane-air explosions exceed the indices of cornstarch explosions by 97% and 80% for ignition delays of 0.65 s and 0.55 s, respectively, resulting in significantly higher hazards.

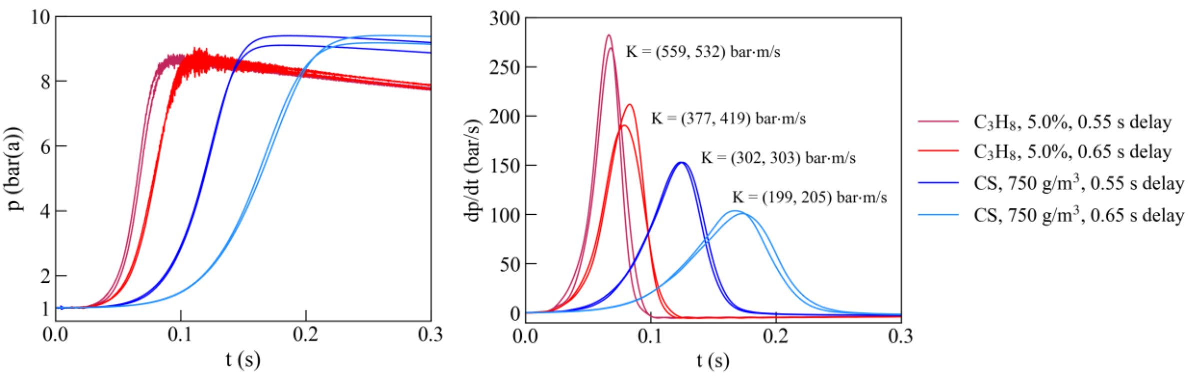

Figure 2: Comparison of turbulent dust (cornstarch, CS) and gas (propane, C_3H_8) explosions. Left: Pressure-time histories. Right: Rate of pressure rise and deflagration index, K.

4 Effect of Elevated Initial Turbulence on Propane-Air Explosions

Following the initial comparison of turbulent dust and gas explosions, a series of gas explosion experiments were performed to characterize explosion dynamics as a function of turbulent fluctuation velocity. The air cannon pressure was reduced to 2.75 bar(g) for these tests, which improved the test repeatability. Fluctuation velocity was measured using a bidirectional probe located at the center of the vessel in unignited tests; measurements were taken with both horizontal and vertical probe orientations to capture possible anisotropic turbulence.

Figure 3 shows the rms (root mean square) of the velocity fluctuations as a function of time (measured from the beginning of injection) for horizonal and vertical probe orientations. Three tests were performed for each probe orientation. Before injection (t = –0.4 s), the signal noise floor is equivalent to about 0.03 m/s. At the end of injection, at t = 0.3 s, fluctuation velocities as high as 4–5 m/s are measured, decaying exponentially until about t = 5 s. During this period, the decay can be approximated as $u'_{rms} = 10^{0.75-0.36t}$. At later times, the rate of decay appears to slow, which may, however, be affected by the noise floor of the measurement. Horizontal and vertical probe orientations do not show any systematic differences.

Turbulent explosion tests were conducted with ignition delays of 0.4 s, 0.6 s, 1.0 s, 2.0 s, and 10 s. In addition, nominally quiescent tests were performed, without air injection and a settling time of 120 s after the end of mixture preparation. All tests used 4.0% propane-air mixtures and a 100-J electric match as an ignition source.

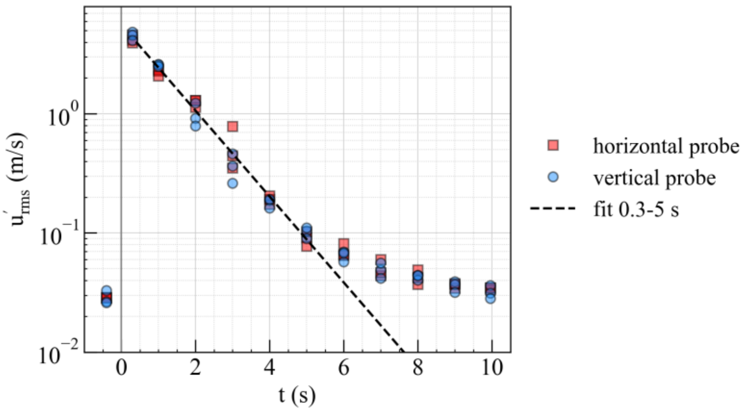

Figure 3: Turbulent fluctuation velocity as a function of time after the beginning of air injection.

Pressure-time histories and rate of pressure rise curves are shown in Fig. 4. Shortening the ignition delay results in faster combustion across the entire range of ignition delays. The slight variations in peak pressure between tests are due to variations in initial vessel temperature. The longest delay, 10 s, yields only marginally faster combustion than the nominally quiescent condition. The profiles of *dp/dt* show a characteristic double-peak for low initial turbulence with ignition delays of 2 s or longer. The first peak is believed to signify the interaction between the flame and the vessel side-walls, temporarily slowing down the flame surface-area growth and increasing the heat loss, and the second peak marks the subsequent growth of flame surface area toward the upper and lower vessel regions. For ignition delays of 1 s or less, the two peaks merge into a single peak as the explosion timescales shorten and heat loss exhibits a lesser effect.

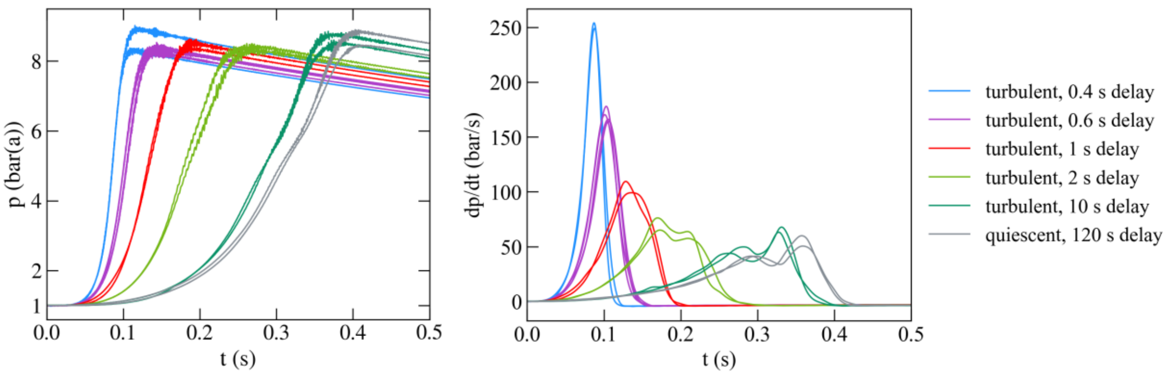

Figure 4: Propane-air explosions under initially turbulent and quiescent conditions. Left: Pressure-time histories. Right: Rate of pressure rise.

Figure 5, left panel, summarizes the deflagration indices, *K*, of all turbulent gas explosion tests performed in this series as a function of turbulent fluctuation velocity, which are evaluated both at the time of ignition (blue circular markers) and at the time of maximum rate of pressure rise (red square markers). *K* increases non-linearly from 125–134 bar·m/s for a 10-s ignition delay ($u'_{rms} \leq 0.03$ m/s; for comparison: 100–119 bar·m/s for quiescent condition after a 120 s delay) to 494–503 bar·m/s for a 0.4 s delay. Turbulence decays only slightly between the time of ignition and the time of maximum rate of pressure rise.

In addition, the early burning velocity, *S*, was estimated by fitting Eq. (2) [8] to the measured pressure-time histories,

$$\Delta p^{1/3} = \left[p_0 \frac{4\pi}{3V}\left(\frac{p_{max}}{p_0} - 1\right)\left(\frac{p_{max}}{p_0}\right)^2\right]^{1/3} S\, t \tag{2}$$

where p_0 is the initial pressure and $p_{\max}$ is the constant-volume explosion pressure. Equation (2) was evaluated in a range of 0.02 bar(g) < Δp < 0.1 bar(g), a range where explosion protection systems such as explosion suppression and active explosion isolation systems would typically activate.

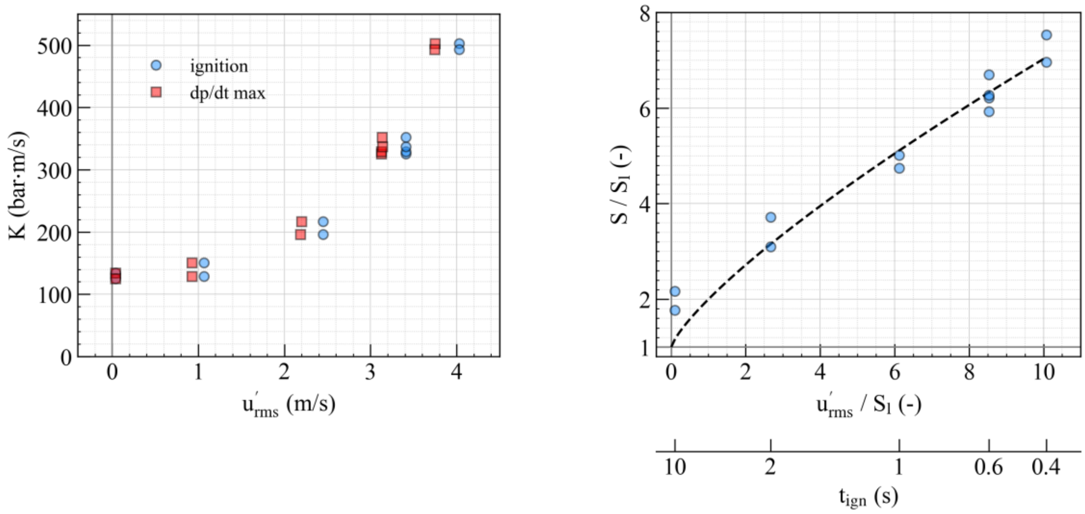

Figure 5: Summary of explosion parameters. Left: Deflagration index, *K*. Right: Early burning velocity, *S*, normalized by the laminar burning velocity, S_l = 0.40 m/s.

Figure 5, right panel, summarizes early burning velocities, *S*, normalized by the laminar unstretched burning velocity of a 4.0% propane-air mixture, S_l = 0.40 m/s [9], as a function of normalized turbulent fluctuation velocity at the time of ignition, or ignition delay. The normalized burning velocity at near-quiescent conditions exceeds the laminar (unstretched) value of 0.4 m/s due to stretch, flame-instability, and ignition effects. The trend between all measurements can be approximated by

$$\frac{S}{S_l} = 1 + \left(\frac{u'_{rms}}{S_l}\right)^{0.78}. \tag{3}$$

This relation is valid for the present mixture within the investigated range of fluctuation velocities, and for the present experimental scale and range of pressures considered when evaluating Eq. (2).

Clearly, *K* and *S* scale differently as a function of initial turbulence. Equation (2) provides the relation between the rate of pressure rise and the burning velocity of a spherical flame neglecting compression effects (applicable during the early stage of an explosion), $S \propto \Delta p^{1/3}/t$. At later times, such as at the time of maximum rate of pressure rise where *K* is determined, this relation is modified by compression effects. Furthermore, flame-wall interactions influence the late stages of the explosion and affect the scaling of *K* as a function of initial turbulence, whereas these effects do not affect the scaling of the early burning velocity, *S*. The results demonstrate that, when using reactivity parameters such as *K* or *S* to assess the hazards of a turbulent explosion or to design explosion protection, it is critical to consider the appropriate scaling of each individual parameter as a function of turbulent fluctuation velocity.

5 Concluding Remarks

This study examined the dynamics of confined gas and dust explosions at large scale under varying levels of initial turbulence. For similar turbulent fluctuation velocities, it was found that propane-air gas explosions produce significantly higher rates of pressure rise than optimal concentrations of cornstarch. Furthermore, it was demonstrated that for gas explosions the scaling of the initial burning velocity with turbulence is significantly different than the scaling of maximum rate of pressure rise. The appropriate scaling for each individual parameter needs to be considered when assessing the hazards of turbulent explosions or designing explosion protection.

Future work will investigate explosions of hybrid mixtures, combining combustible dusts and flammable gases, in a range of turbulence levels relevant to industrial explosions.

References

[1] Ciccarelli G, Dorofeev S. (2008). Flame acceleration and transition to detonation in ducts. Prog. Energ. Combust. 34: 499.

[2] Bradley D, Chamberlain GA, Drysdale DD. (2012). Large vapour cloud explosions, with particular reference to that at Buncefield. Phil. Trans. R. Soc. A. 370: 544.

[3] Houim R, Oran ES. (2015). Numerical simulation of dilute and dense layered coal-dust explosions. Proc. Combust. Inst. 35: 2083.

[4] Tamanini, F. (1998). The role of turbulence in dust explosions. J. Loss Prevent. Proc. 11: 1.

[5] Scheid M, Geissler A, Krause U. (2006). Experiments on the influence of pre-ignition turbulence on vented gas and dust explosions. J. Loss Prevent. Proc. 19: 194.

[6] Proust C, Leprette E, Snoeys J. (2011). The role of turbulence in explosion vent system design. Hazards XXII, Process Safety and Environmental Protection, Symposium Series 156. Institution of Chemical Engineers UK.

[7] McCaffrey BJ, Heskestad G. (1976). A robust bidirectional low-velocity probe for flame and fire applications. Combust. Flame. 26: 125.

[8] Nagy J, Conn JW, Verakis HC. (1969). Explosion development in a spherical vessel. US Department of the Interior, Bureau of Mines. Vol. 7279.

[9] Vagelopoulos CM, Egolfopoulos FN, Law CK. (1994). Further considerations on the determination of laminar flame speeds with the counterflow twin-flame technique. Proc. Combust. Inst. 25: 1341.